

# Microbial Reduction of Graphene Oxide by *Lactobacillus Plantarum*

Güldem Utkan<sup>1,\*</sup>, Tarik Öztürk<sup>2</sup>, Özgür Duygulu<sup>3</sup>, Elif Tahtasakal<sup>4</sup> and Aziz Akin Denizci<sup>4</sup>

<sup>1</sup>Department of Chemical Engineering, Faculty of Engineering, Marmara University, Istanbul, Turkey.

<sup>2</sup>Food Institute, Marmara Research Center, TUBITAK, Kocaeli, Turkey.

<sup>3</sup>Materials Institute, Marmara Research Center, TUBITAK, Kocaeli, Turkey.

<sup>4</sup>Genetic Engineering and Biotechnology Institute, TUBITAK, Marmara Research Center, Kocaeli, Turkey.

(\*) Corresponding author: [guldem.utkan@marmara.edu.tr](mailto:guldem.utkan@marmara.edu.tr)

(Received: 31 January 2018 and Accepted: 15 January 2019)

## Abstract:

Here, we report that the reduced graphene oxide nanosheets were successfully synthesized using the *Lactobacillus plantarum* biomass in a simple, environmentally friendly and scalable manner. We produced graphene oxide by oxidization and exfoliation of graphite flakes with modified Hummer's method and then reduced to reduced graphene oxide by using *Lactobacillus plantarum* biomass as a reducing agent. Samples were characterized using Fourier transform infrared spectroscopy, X-ray photoelectron spectroscopy, transmission electron microscopy, scanning electron microscopy, microconfocal raman spectroscopy and thermogravimetric analysis. After the reduction, we observed that a considerable decrease in the oxygen containing functional groups of graphene oxide and an increase in C/O ratio from 1.7 to 3.3 in which confirms sp<sup>2</sup> graphitic carbons increase. Mainly, we observed a significant decrease in epoxy and alkoxy functionalities. Furthermore, we determined an exfoliation of graphene oxide to one or several (2-5) layers after the complete reduction. In addition to reducing potential, *Lactobacillus plantarum* biomass also plays an important role as stabilizing agent; here the reduced graphene oxide showed a good stability in water. The green synthesis reported in this work is concerned with the production of high purity water-dispersible reduced graphene oxide using *Lactobacillus plantarum* CCM 1904.

**Keywords:** Graphene, Microbial reduction, 2D material, *Lactobacillus*.

## 1. INTRODUCTION

Recently, graphene has attracted great interest of researchers in materials world, since it has excellent mechanical [1], thermal [2], electrical [3] and optical [4,5] properties coming from its two dimensional structure [6] for various applications, such as super-capacitors, batteries, fuel cells, solar cells, hydrogen storage, reinforcement of polymer, ceramic and metal matrix composites, conductive paints and inks, drug delivery, biosensors etc. [7-13]. The most recent applications related with graphene and graphene related substances are graphene oxide modified photocatalysts [14], preparation of

biodegradable bionanocomposites [15], graphene humidity sensors [16], gas separation [17] electrochemical energy storage devices [18], graphene-based flexible and stretchable bioelectronics in health care systems [19], and dye-sensitized solar cells [20]. Growing increase in applications of these materials are also necessitates the development of new strategies for mass production.

In the literature, there are some strategies reported to synthesize graphene such as micro - mechanical exfoliation of graphite [21], epitaxial growth [22-24], chemical vapour deposition [23,25,26] etc. Although all

of these methods have their own advantages and disadvantages, achieving a stable dispersion and scalability in the preparation of the graphene is a major problem. One of the most effective way of a large scale graphene production have been based on oxidative-exfoliation of graphite to graphene oxide (GO) and then additional treatments to reduce it to reduced graphene oxide (RGO) [6, 21, 24, 28-44].

Main research should focus on advancement of reduction processes which keep the structure and properties of pristine graphene. That means, it is important to reduce the graphene oxide so as to recover the honeycomb hexagonal lattice of graphene. The exact process parameters used when reducing GO into rGO play a major role in the quality of the material, affecting how close a structure to perfect graphene is achieved. Applying different reduction processes produces reduced graphene oxide (RGO) in different properties which finally affect the performance of materials and devices built up from RGO. In terms of mass production of graphene, the chemical reduction of graphene oxide is considered to be one of the most viable methods. However, scientists have found it challenging to create graphene sheets that have the same quality as those made by mechanical exfoliation on a large scale. Chemical [45-48], electrochemical [49,50] and thermal [51] reductions are the mostly reported reduction processes.

When large-scale production is considered, these methods bring some economical and/or chemical reduction requires hydrazine like strong reducing agents, and toxic or/and corrosive concentrated alkaline solutions, thermal reduction requires very high temperatures and special reactors and electrochemical reduction consumes too much energy and requires expensive electrodes. These disadvantages put forward the search of new strategies for reduction of GO under

mild and environmentally benign conditions [48,52,53]. Researchers are now concentrating on reduction of GO by biological methods as a new strategy.

Microbial reduction among the other biological methods is an exciting new area to develop a considerable potential for reduction of GO. A number of microbial species would be able to use as reducing agent. Some microorganisms, bacteria, like *Shewanella* [54,55], *E. coli* [56,57], have been utilized for reducing oxides on the edges of GO. Yeast *Candida albicans* A.T.C.C. 10231 was also reported for reduction of graphene oxide to graphene [58]. In another work, reducing ability of baker's yeast towards ketones on graphene oxide has been reported [59].

In this work, we report a simple and eco-friendly strategy to obtain reduced graphene oxide by using *Lactobacillus plantarum* as reducing agent. In this green route, large scale production of stable dispersions of reduced graphene oxide is possible.

## 2. EXPERIMENTAL

### 2.1 Materials

All chemicals were purchased from Sigma-Aldrich (USA) as analytical grade and used directly without further purification. All aqueous solutions were prepared with deionized water. Graphite (92% graphitic carbon content) flake was supplied from Syrah Resources (Australia).

### 2.2 Preparation of Biomass

*Lactobacillus plantarum* CCM 1904 was supplied from Czech Collection of Microorganisms. The preculture (5 ml of CCM medium no 6 in 25 ml flask) was inoculated with a single colony of *Lactobacillus plantarum* CCM 1904 and incubated on a rotary shaker at 30°C for 18 h. The second precultures were inoculated with the first preculture (1% v/v) and incubated on a rotary shaker 30°C for 24 h in 150 ml batch

medium in 500 ml shake flasks. The cells were harvested by centrifugation, washed twice with phosphate-buffered saline (pH 7.3) and 720 mg wet cells collected in a 50-ml tube and further used for synthesis of reduced graphene.

### 2.3 Graphene Oxide Synthesis

GO was prepared from flake graphite using modified Hummer's method [43] given by Gurunathan et al [57]. In a typical preparation, 2 g of graphite powder was mixed with 80 mL H<sub>2</sub>SO<sub>4</sub> and 20 mL HNO<sub>3</sub> in an ice bath, and then 12 g KMnO<sub>4</sub> was very slowly added. After KMnO<sub>4</sub> addition, the solution heat was raised to 35 °C for 30 min and 160 mL deionized water was added for dilution and rested for 1 h. Further dilution was achieved by addition of 400 mL deionized water, followed by slow addition of 12.0 mL of H<sub>2</sub>O<sub>2</sub> (30% v/v) and black graphite suspension was turned to yellow graphite oxide solution after these procedures. After centrifugation at 3000 rpm/min for 15 min, the graphite oxide precipitate was obtained and washed with deionized water. Pellet was re-suspended in water and aqueous solution of graphite oxide was obtained.

A few layer graphene oxide nanosheets in an aqueous solution (dark brown in color) (6 mg/ml) was prepared by application of 2 hr sonification to graphite oxide solution for exfoliation of layers.

### 2.4 Reduction of Graphene Oxide and Purification of Reduced Graphene

The reduction experiment, 200 mg of *Lactobacillus plantarum* CCM 1904 biomass was added to the GO dispersion (0.5 mg/ml), and the mixture was incubated at 30°C for in static conditions for 1 week. After reduction, the stable black dispersion was sonicated for 5 min to disperse the cells from graphene materials and then

centrifuged at 10,000 rpm/min for 10 min to remove bacteria as a supernatant liquid. The black pellet was resuspended in water. Further purification steps continued with washing 80% ethanol and 1N HCl including water washings between the steps and final water washing step until neutralization were obtained according to method given by Salas et al [54].

After completing washing steps, samples were lyophilized. The obtained black dispersion was designated as *Lactobacillus plantarum* CCM 1904 reduced graphene oxide (RGO) and used for further characterization.

### 2.5 Characterization of GO and RGO

The morphology of the samples was analysed using JEOL JSM 6335F high resolution scanning electron microscope (HRSEM). HRTEM (high resolution transmission electron microscopy) was used for more detailed analysis. Transmission electron microscopy investigations were performed on JEOL JEM 2100 HRTEM operating at 200 kV. Images were taken by Gatan Model 794 Slow Scan CCD Camera and also by Gatan Model 833 Orius SC200D CCD Camera. Carbon support film coated copper TEM grids (Electron Microscopy Sciences, CF200-Cu, 200 mesh) were used.

Fourier transformed infrared spectroscopy (FT-IR) was carried out on a Shimadzu IR Prestige 21, for which samples were prepared in potassium bromide (KBr) pellets.

For X-ray photoelectron spectrometer (XPS) analysis, the control and test samples were mounted on a carbon tape and recorded the XPS spectra using a Thermo Scientific K-Alpha X-ray photoelectron spectrometer. Monochromatized Al K $\alpha$  radiation (Al K $\alpha$  = 146.3 eV) was used as the X-ray source and flood gun was used for charge compensation during the measurements. The X-ray spot size was

approximately 400  $\mu\text{m}$ . Electron take-off angle between the sample surface and the axis of the analyzer lens was set to  $90^\circ$ . Spectra were recorded using Avantage 5.9 data system. The binding energy scale was calibrated by assigning the C1s signal at 284.5 eV.

Microconfocal Raman spectra were recorded from 200 to  $3000\text{ cm}^{-1}$  on a Renishaw Invia Raman Microprobe by using a 532 nm argon ion laser.

Thermogravimetric analysis (TGA) of graphene oxide and reduced graphene was carried out under  $\text{N}_2$  flow using TA Instrument Thermogravimetric Analyzer Q50 (USA) and their masses were recorded as a function of temperature. The samples were heated from room temperature to  $600\text{ }^\circ\text{C}$  at  $5\text{ }^\circ\text{C}/\text{min}$ .

### 3. RESULTS AND DISCUSSION

GO was produced by modified Hummers' method [43]. In this method, graphite powder was first oxidized to graphite oxide by using  $\text{KMnO}_4/\text{H}_2\text{SO}_4$  and GO nanosheets were formed by ultrasonification. The obtained GO has dark brown color and kept its stability more than 6 months in water, which is attributed to high number of hydrophilic functional groups existing on and at the edges of GO nanosheets. RGO was produced by microbial reduction. For this reason, the biomass of *Lactobacillus plantarum* CCM 1904 was added into the GO dispersion and kept in static condition at  $30\text{ }^\circ\text{C}$  for a week. After reduction, color changed to black and precipitated since there was a huge decrease in number of functional groups which causes a loss in dispersion stability. The reduction of GO by *Lactobacillus plantarum* CCM 1904 was confirmed by control experiment designed without bacterial biomass. In control experiment, color of GO dispersion did not change after it kept at  $30\text{ }^\circ\text{C}$  in static culture for a week. It is determined that

*Lactobacillus plantarum* CCM 1904 biomass plays an important role in the GO reduction.

Besides the visibility observations in color change, the presence of different type of oxygen functionalities in GO and RGO, as well as reduction, were determined by FT-IR analysis.

FTIR spectrum of GO and RGO was given in Fig. 1. The following characteristic peaks were observed ( $\text{cm}^{-1}$ ) for GO: 3410(s) O-H stretching from alkoxy and carboxyl groups, 1636(m) C=O stretching vibration of carboxylic acid, 1528 (w) C=C skeletal vibration of the graphene planes (aromatic ring), 1396(w) C-O vibrational stretching of carboxylic acid or deformation vibration of tertiary alcohol, 1211 (m) and 1159 (w) epoxy C-O stretching vibrational bands, 1103(m) and 1057(m) alkoxy C-O stretching, 872(m), 674 (m) and 586 (m) aromatic  $\text{sp}^2$  C-H bending vibrations. FTIR peak of RGO presents that O-H stretching vibrations observed at  $3387\text{ cm}^{-1}$  was significantly reduced, however there were still O-H coming from water absorbed. 1636 (m) peak moved to  $1643\text{ cm}^{-1}$  and oxygen coming from carboxylic acid was decreased. After reduction, the peaks for oxygen-containing groups significantly decreased or disappeared and the characteristic peak of C=C stretching vibration at  $1535\text{ cm}^{-1}$  increased. Vibrational stretching of carboxylic acid or deformation vibration of tertiary alcohol C-O peak at  $1388\text{ cm}^{-1}$  remained the same. 1211 (m) C-O epoxy stretching vibrational band was significantly decreased and almost disappeared. 1159 (w), 1103(m) and 1057(m) C-O stretching bands were disappeared due to reduction process and a single C-O (m) vibrational stretching band at  $1096\text{ cm}^{-1}$  was formed from remaining carboxyl or alkoxy groups. The peak at  $870\text{ cm}^{-1}$  was remained the same, however 671

$\text{cm}^{-1}$  and  $586 \text{ cm}^{-1}$  were formed a new single peak at  $664 \text{ cm}^{-1}$  which was attributed to aromatic  $\text{sp}^2$  C-H bending [60].

Chemical structure of GO and RGO were further examined with XPS as shown in Fig. 2. The C 1s XPS spectrum of GO clearly shows that there are peaks correspond to carbon atoms in different functional groups:

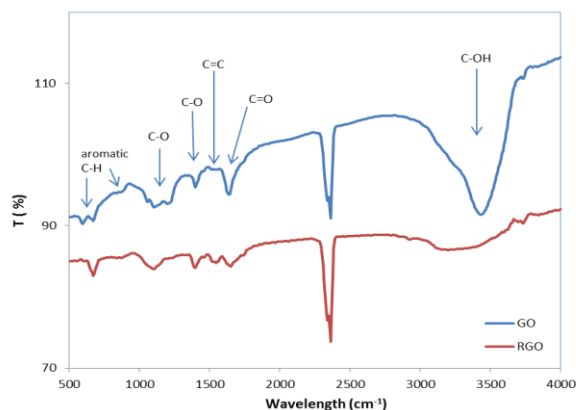


**Figure 1.** FT-IR analysis of GO and RGO.

Non-oxygenated C in C-C (284.3 eV), the C in C-OH bonds (286.07 eV), C-O-C (286.6 eV), C=O (287.76 eV), O-C=O (288.8 eV). Also, after reduction C 1s XPS spectrum of RGO binding energy at 284.3 eV for C-C, 285.9 eV for C-OH, 286.6 eV for C-O, 287.6 eV for C=O, 288.97 eV for O-C=O. Although the RGO has the same oxygen functional group peaks at C1s XPS spectrum, their intensities were reduced significantly as seen in Figure 2.

This reduction showed that microorganisms were very effective for the reduction process through C-O-C and C-OH functional groups compared to C=O and C-O=O groups. This noticeable reduction in C1s peak intensities of C-OH, C-O-C, C=O, C-O=O groups are consistent with the results of FTIR spectra reported.

Atomic ratio of carbon to oxygen (C/O) was also calculated for both GO and RGO by taking ratio of C 1s to O

1s peak areas in XPS spectra. It was observed that the C/O ratio increased from 1.7 to 3.3 after microbial reduction. It can be speculated that 51.5% increase in C/O ratio after reduction comes from decrease in intensity of C-OH and C-O-C at the same time increase in C-C  $\text{sp}^2$  bond as a result of removal of oxygen groups.

It was reported that C-OH and C=O peak intensities were decreased considerable amount by chemical reduction and biological reduction by *Shewanella* [54]. There was no indication of any epoxy and carboxyl groups in the reacted samples by *Shewanella* [54]. After reduction of GO with baker's yeast, there was a dramatic decrease in the oxygen functionalities such as -COOH and -OH, a slight decrease in epoxy and no change in alkoxy were observed [59]. A change in C=O bands in GO by *E. coli* reduction was reported [57]. In this study, it was seen that reduction of GO with *Lactobacillus plantarum* CCM 1904 was very effective in reducing epoxy and alkoxy functionalities.

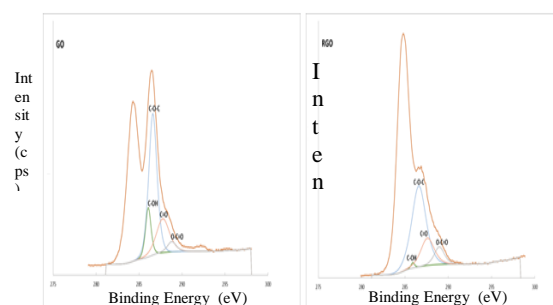


**Figure 2.** XPS analysis of GO and RGO.

Additionally, Raman spectroscopy was used to monitor structural changes in the oxidation and reduction processes. Raman spectroscopy analysis is sensitive to electronic structure and valuable tool for characterization of carbon-based materials having high Raman intensity by C=C in their structure [61]. Typical Raman spectra of graphene has a prominent peak at  $1580 \text{ cm}^{-1}$  (G band) attributed to the  $\text{E}_{2g}$

phonon of C  $sp^2$  atoms and  $1350\text{ cm}^{-1}$  (D band) originated from a second-order overtone of a different in-plane vibration [62].

In this study, both GO and RGO samples were deposited on glass slide as thin layer and dried at room temperature. Fig. 3 showed the Raman spectra of both GO and RGO which had two major peaks at G and D bands. These two bands were broader in GO than those in RGO as a result of higher disorder in GO. The higher intensity and sharper bands in RGO corresponded to the restoring C-C  $sp^2$  domains as well as addition of new C-C  $sp^2$  network after the reduction process. The spectrum of GO had peaks at  $1365$  and  $1613\text{ cm}^{-1}$  which were corresponding to D and G bands, respectively. D band indicated decrease in average size of in-plane  $sp^2$  domain of GO or RGO originating from defects [63]. The intensity of ratio of D band to G band ( $I_D/I_G$ ) of GO was about 0.94. The D and G bands shifted to  $1360$  and  $1608\text{ cm}^{-1}$  and its  $I_D/I_G$  decreased to 0.92 due to removal of oxygen functional groups during the reduction. This result suggested that RGO has less defect compared to GO. After reduction,  $5\text{ cm}^{-1}$  shift decrease in G band suggests us that the numbers of graphene layers are around 2-5.

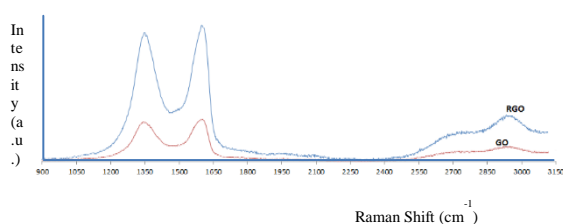


**Figure 3.** Raman spectra of GO and RGO.

Thermal stability of GO and RGO were investigated with TGA analysis. It was showed that GO decomposes with one clear step at  $162\text{ }^\circ\text{C}$  with total weight loss of 85.9% in Fig. 4. A significant decrease in mass was observed at  $162\text{ }^\circ\text{C}$ . The

major mass reduction was caused by pyrolysis of the oxygen-containing functional groups, generating CO, CO<sub>2</sub> and steam. However, the RGO exhibited slight two step decomposition of oxygen containing groups at  $207.3\text{ }^\circ\text{C}$  and  $289.6\text{ }^\circ\text{C}$  with total weight loss of 62.2%. Smaller weight loss of RGO compared to GO could be explained by decrease in oxygen containing functional groups amount after reduction which enhances the thermal stability of the material.

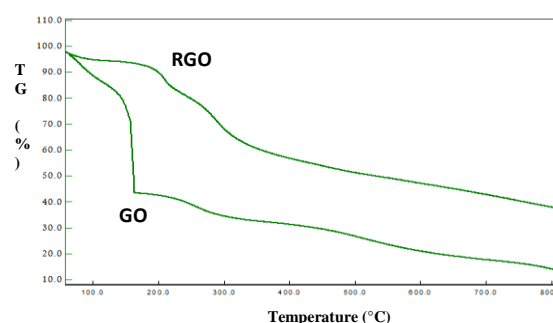


**Figure 4.** TGA analysis of GO and RGO.

The morphology and structure of GO and RGO were analyzed by SEM and TEM observations.

Fig. 5 showed SEM image of RGO nanosheets in flaky, layered, irregular and folding structure at the edges. They are entangled with each other. They are transparent and have rippled leaf-like morphology. They have rough surface.

In Fig. 6, TEM image of GO, a few layer of independent GO nanosheets with size of  $2\text{ }\mu\text{m}$  were observed. They are flat since van der Waals interactions between GO layers were broken during the sonification process and sample preparation and they have large amount of oxygen-containing functional groups on their surfaces. Mostly a single or a few (2-5) layer RGO nano sheets with some wrinkles were observed in TEM images as shown in Fig. 6.

Genes that encode a bd-type cytochrome (cydABCD) were identified in the genome of *Lactobacillus plantarum*.

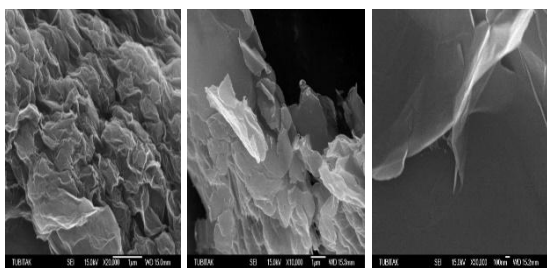


**Figure 5.** SEM image of RGO nanosheets obtained from different regions.

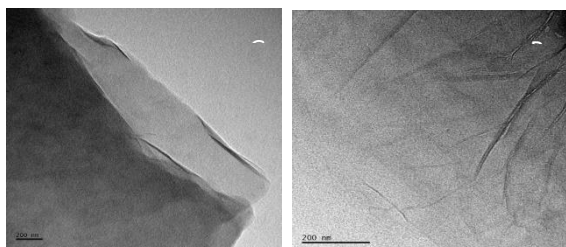


**Figure 6.** TEM images of GO and RGO.

The existence of a non-redundant branched electron transport chain in *Lactobacillus plantarum* WCFS1 was proposed that was capable of using oxygen or nitrate as terminal electron acceptor [64]. The possible mechanism of synthesis of graphene by bacteria involves cell trapping or electron mediators [57].

We speculate that bd-type cytochrome (cydABCD) exists in *Lactobacillus plantarum* CCM 1904 genome plays an important role in reduction process of GO by providing electron transport. Further research should focus on electron transport mechanism of *Lactobacillus plantarum* CCM 1904

and reduction-responsible genes should be shown.

#### 4. CONCLUSIONS

In this study, we have successfully showed that GO could be efficiently reduced by *Lactobacillus plantarum* CCM 1904 biomass. Reduction process does not need any toxic chemicals and harsh process conditions. The reduction was carried out in aqueous medium at 30°C. Efficiency of reduction processes were confirmed by TEM, XPS and microconfocal Raman spectroscopy.

The results showed that *Lactobacillus plantarum* CCM 1904 is very affective for the reduction of GO and RGO forms clear graphene nanosheets dispersible in water. Further study should focus on the electron transport mechanism of *Lactobacillus plantarum* during the reduction of GO.

This eco-friendly and simple approach opens up the possibility of production of graphene in large scale.

#### CONFLICT OF INTEREST

The authors declare that there is no conflict of interest regarding the publication of this paper

#### ACKNOWLEDGEMENT

We thank Dr. Uğur Unal, Koc University for performing XPS analysis.

#### REFERENCES

1. Lee, C. G., Wei, X. D., Kysa, J. W., Hone, J., (2008). "Measurement of the elastic properties and intrinsic strength of monolayer graphene", *Science*, 321: 385-388.
2. Balandin, A. A., Ghosh, S., Bao, W., Calizo, I., Teweldebrhan, D., Miao, F., Lau, C. N., (2008). "Superior thermal conductivity of single-layer graphene", *Nano Letters*, 8: 902-907.
3. Orlita, M., Faugeras, C., Plochocka, P., Neugebauer, P., Martinez, G., Maude, D. K., Barra, A. L., Sprinkle, M., Berger, C., De Heer, W. A., Potemski, M., (2008). "Approaching the dirac point in high mobility multilayer epitaxial graphene", *Physical Review Letter*, 101: 267601.
4. Cai, W., Zhu, Y., Li, X., Piner, R. D., Ruoff, R. S., (2009). "Large area few-layer graphene/graphite films as transparent thin conducting electrodes", *Applied Physical Letters*, 95: 123115.
5. Li, X., Zhu, Y., Cai, W., Borysiak, M., Han, B., Chen, D., Piner, R. D., Colombo, L., Ruoff, R. S., (2009). "Transfer of large-area graphene films for high-performance transparent conductive electrodes", *Nano Letters*, 9: 4359-4363.
6. Geim, K. A., Novoselov, K. S., (2007). "The rise of graphene", *Nature Materials*, 6: 183-191.

7. Liu, Z., Lau, S. P., Yan, F., (2015). "Functionalized graphene and other two-dimensional materials for photovoltaic devices: device design and processing", *Chemical Society Reviews*, 44: 5638-5679.
8. Xia, F., Mueller, T., Lin, Y. M., Valdes-Garcia A., Avouris, P., (2009). "Ultrafast graphene photodetector", *Nature Nanotechnology*, 4: 839-843.
9. Liu, M., Zhang, R., Chen, W., (2014). "Graphene-supported nanoelectrocatalysts for fuel cells: synthesis, properties, and applications", *Chemical Reviews*, 114: 5117-5160.
10. Wu, Z. S., Feng, X., Cheng, H. M., (2013). "Recent advances in graphene-based planar micro-supercapacitors for on-chip energy storage", *National Science Reviews*, 1: 277-292.
11. Zhai, Y., Dou, Y., Zhao, D., Fulvio, F. P., Mayes, R. T., Dai, S., (2011). "Carbon materials for chemical capacitive energy storage", *Advanced Materials*, 23: 4828-4850.
12. Liu, Y., Dong, X., Chen, P., (2012). "Biological and chemical sensors based on graphene materials", *Chemical Society Reviews*, 4: 2283-2307.
13. Mao, H. Y., Laurent, S., Chen, W., Akhavan, O., Imani, M., Ashkarran, A. A., Mahmoudi M., (2013). "Graphene: promises, facts, opportunities, and challenges in nanomedicine", *Chemical Reviews*, 113: 3407-3424.
14. Kumar, S., Yadav, R. K., Ram, K., Aguiar, A., Koh, J., Sobral, A. J. F. N., (2018). "Graphene oxide modified cobalt metallated porphyrin photocatalyst for conversion of formic acid from carbon dioxide", *Journal of CO<sub>2</sub> Utilization*, 27: 107-114.
15. Kumar, S., Koh, J., (2014). "Physiochemical and optical properties of chitosan based graphene oxide bionanocomposite", *International Journal of Biological Macromolecules*, 70: 559-564.
16. Raccichini, R., Varzi, A., Passerini, S., Scrosati, B., (2015). "The role of graphene for electrochemical energy storage", *Nature Materials*, 14: 271-279.
17. Azamat, J., (2018). "Application of Functionalized Graphene Oxide Nanosheet in Gas Separation", *International Journal of Nanoscience and Nanotechnology*, 14: 165-175.
18. Kumar, V., Khandelval, G., (2016). "Graphene-based Flexible and Stretchable Bioelectronics in Health Care Systems", *Journal of Analytical and Pharmaceutical Research*, 3: 53-55.
19. Roy-Mayhew, J. D., Aksay, I. A., (2014). "Dye-Sensitized Solar Cells", *Chemical Reviews*, 114: 6323-6348.
20. Smith, A.D., Elgammal, K., Niklaus, F., Delin, A., Fischer, A. C., Vaziri, S., Forsberg, F., Rasander, M., Hugosson, H., Berqvist, L., Schröder, S., Kataria, S., Östling, M., Lemme, M. C., (2015). "Resistive graphene humidity sensors with rapid and direct electrical readout", *Nanoscale*, 7: 1909919109.
21. Geim, A. K., (2009). "Graphene: status and prospects", *Science*, 324: 1530-1534.
22. Novoselov, K. S., Geim, A. K., Morozov, S. V., Jiang, D., Zhang, Y., Dubonos, S. V., Grigorieva, I. V., Firsov, A. A., (2004). "Electric field effect in atomically thin carbon films", *Science*, 306: 666-669.
23. Berger, C., Song, Z., Li, X., Wu, X., Brown, N., Naud, C., Mayou, D., Li, T., Hass, J., Marchenkov, A. N., Conrad, E. H., First, P. N., De Heer, W. A., (2006). "Electronic confinement and coherence in patterned epitaxial graphene", *Science*, 312: 1191-1196.
24. Wintterlin, J., Bocquet, M. L., (2009). "Graphene on metal surface", *Surface Science*, 603: 1841-1852.
25. Land, T. A., Michely, T., Behm, R. J., Hemminger, J. C., Comsa, G., (1992). "STM investigation of single layer graphite structures produced on Pt (111) by hydrocarbon decomposition", *Surface Science*, 264: 261-270.
26. Eizenberg, M., Blakely, J. M., (1979). "Carbon monolayer phase condensation on Ni (111)", *Surface Science*, 82: 228-236.
27. Kim, K. S., Zhao, Y., Jang, H., Lee, S. Y., Kim, J. M., Kim, K. S., Ahn, J. H., Kim, P., Choi, J. Y., Hong, B. H., (2009). "Large scale pattern growth of graphene films for stretchable transparent electrodes", *Nature*, 457: 706-710.
28. Sakamoto, J., Van Heijst, J., Lukin, O., Schluter, A. D., (2009). "Two dimensional polymers: just a dream of synthetic chemists?", *Angewandte Chemie International Edition*, 48: 1030-1069.
29. Regis, Y. N. G., Spyrou, K., Rudolf, P., (2010). "A roadmap to high quality chemically prepared graphene", *Journal of Physics D*, 43: 374015-374034.
30. Compton, O. C., Nguyen, S. T., (2010). "Graphene oxide, highly reduced graphene oxide, and graphene: versatile building blocks for carbon-based materials", *Small*, 6: 711-723.
31. Park, S., Ruoff, R. S., (2009). "Chemical methods for the production of graphenes", *Nature Nanotechnology*, 4: 217-224.
32. Zhu, Y., Murali, S., Cai, W., Li, X., Suk J. W., Potts, J. R., Ruoff, R. S., (2010). "Graphene and Graphene oxide: synthesis, properties and applications", *Advanced Materials*, 22: 3906-3924.
33. Huang, X., Yin, Z., Wu, S., Qi, X., He, Q., Zhang, Q., Yan, Q., Boey, F., Zhang, H., (2011). "Graphene based materials: synthesis, characterization, properties, and applications", *Small*, 7: 1876-1902.
34. Guo, S., Dong, S., (2011). "Graphene nanosheet: synthesis, molecular engineering, thin film, hybrids, and energy and analytical applications", *Chemical Society Review*, 40: 26442672.



35. Neto, A. H. C., Guinea, F., Peres, N. M. R., Novoselov, K. S., Geim, A. K., (2009). "The electronic properties of graphene", *Reviews of Modern Physics*, 81: 109-162.
36. Geim, A. K., MacDonald, A. H., (2007). "Graphene: exploring carbon flatland", *Physics Today*, 60: 35-41.
37. Katsnelson, M. I., Novoselov, K. S., (2007). "Graphene: new bridge between condensed matter physics and quantum electrodynamics", *Solid State Community*, 143: 3-13.
38. Rao, C. N. R., Sood, A. K., Subrahmanyam, K. S., Govindaraj, A., (2009). "Graphene: the new two-dimensional nanomaterial", *Angewandte Chemie International Edition*, 48: 7752-7777.
39. Loh, K. P., Bao, Q., Ang, P. K., Yang, J., (2010). "The chemistry of graphene", *Journal of Materials Chemistry*, 20: 2277-2289.
40. Boukhvalov, D. W., Katsnelson, M. I., (2009). "Chemical functionalization of graphene", *Journal of Physics: Condensed Matter*, 21: 344205-344217.
41. Allen, M. J., Tung, V. C., Kaner, R. B., (2009). "Honeycomb carbon: a review of graphene", *Chemical Reviews*, 110: 132-145.
42. Huang, X., Qi, X., Boey, F., Zhang, H., (2012). "Graphene-based composites", *Chemical Society Reviews*, 41: 666-686.
43. Hummers, W. S., Offeman, R. E., (1958). "Preparation of graphitic oxide", *Journal of American Chemical Society*, 80: 1339-1339.
44. Farazas, A., Mavropoulos, A., Christofilos, D., Tsiaoussis, I., Tsipas, D., (2018). "Ultrasound Assisted Green Synthesis and Characterization of Graphene Oxide", *International Journal of Nanoscience and Nanotechnology*, 14: 11-17.
45. Fan, X., Peng, W., Li Y., Li, X., Wang, S., Zhang, G., Zhang, F., (2008). "Deoxygenation of exfoliated graphite oxide under alkaline conditions: A green route to graphene preparation", *Advanced Materials*, 20: 4490-4493.
46. Stankovich, S., Dikin, D. A., Piner, R. D., Kohlhaas, K. A., Kleinhammes, A., Jia, Y., Wu, Y., Nguyen, S. T., Ruoff, R. S., (2007). "Synthesis of graphene-based nanosheets via chemical reduction of exfoliated graphite oxide", *Carbon*, 45: 1558-1565.
47. Zhu, C., Guo, S., Fang, Y., Dong, S., (2010). "Reducing sugar: New functional molecules for the green synthesis of graphene nanosheets", *ACS Nano*, 4: 2429-2437.
48. Zhang, J. L., Yang, H. J., Shen, G. X., Cheng, P., Zhang, J. Y., Guo S. W., (2010). "Reduction of graphene oxide via L-ascorbic acid", *Chemical Communications*, 46: 1112-1114.
49. Wang, Z., Zhou, X., Zhang J., Boey, F., Zhang, H., (2009). "Direct electrochemical reduction of single-layer graphene oxide and subsequent functionalization with glucose oxidase", *The Journal of Physical Chemistry C*, 113: 14071-14075.
50. Zhou, M., Wang, Y., Zhai, Y., Zhai, J., Ren, W., Wang, F., Dong, S., (2009). "Controlled synthesis of large-area and patterned electrochemically reduced graphene oxide films", *Chemistry- A European Journal*, 15: 6116-6120.
51. Mcallister, M. J., Li, J., Adamson, H. D., Schnlepp, C. H., Abdalam, A. A., Liu, J., Herrera-Alonso, M., Milius, D. L., Car, R., Prud'homme, R. K., Aksay, I. A., (2007). "Single sheet functionalized graphene by oxidation and thermal expansion of graphite", *Chemistry of Materials*, 19: 4396-4404.
52. Gao, J., Liu, F., Liu, Y., Ma, N., Wang, Z., Zhang, X., (2010). "Environment-friendly method to produce graphene that employs vitamin C and amino acid", *Chemistry of Materials*, 22: 2213-2218.
53. Guo, H., Wang, X. F., Qian, Q. Y., Wang, F. B., Xia, X. H., (2009). "A green approach to the synthesis of graphene nanosheets", *ACS Nano*, 3: 2653-2659.
54. Salas, E. C., Sun, Z., Luttge, A., Tour, J. M., (2010). "Reduction of graphene oxide via bacterial respiration", *ACS Nano*, 4: 4852-4856.
55. Wang, G., Qian, F., Saltikov, C., Jiao, Y., Li, Y., (2011). "Microbial reduction of graphene oxide by *Shewanella*", *Nano Research*, 4: 563-570.
56. Akhavan, O., Ghaderi, E., (2012). "Escherichia coli bacteria reduce graphene oxide to bactericidal graphene in a self-limiting manner", *Carbon*, 50: 1853-1860.
57. Gurunathan, S., Han, J. W., Eppakayala, V., Kim, J. H., (2013). "Microbial reduction of graphene oxide by Escherichia coli: a green chemistry approach", *Colloids and Surfaces B: Biointerfaces*, 102:772-777.
58. Al Ali Alamaadeed, M., (2014). "Simple production method for graphene by microorganisms", Patent No. US20150336799 A1.
59. Khanra, P., Kuila, T., Kim, N. H., Bae, S. H., Yu, D. S., Lee, J. H., (2012). "Simultaneous biofunctionalization and reduction of graphene oxide by baker's yeast", *Chemical Engineering Journal*, 183: 526-570.
60. Tucureanu, V., Matei, A., Avram, A. M., (2016). "FTIR Spectroscopy for Carbon Family Study", *Critical Reviews in Analytical Chemistry*, 46: 502-520.

61. Niyogi, S., Bekyarova, E., Itkis, M. E., Zhang, H., Shepperd, K., Hicks, J., Sprinkle, M., Berger, C., Lau, C. N., De Heer W. A., Conrad, E. H., Haddon, R. C., (2010). "Spectroscopy of covalently functionalized graphene", *Nano Letters*, 10: 4061-4066.
62. Frank, O., Mohr, M., Maultzsch, J., Thomsen, C., Riaz, I., Jalil, R., Novoselov, K. S., Tsoukleri, G., Parthenios, J., Papagelis, K., Kavan, L., Galiotis, C., (2011). "Raman 2D-band splitting in graphene: theory and experiment", *ACS Nano*, 5: 2231-2239.
63. Zhou, Y., Bao, Q., Tang, L. A. L., Zhong, Y., Loh, K. P., (2009). "Hydrothermal dehydration for the "green" reduction of exfoliated graphene oxide to graphene and demonstration of tunable optical limiting properties", *Chemistry of Materials*, 21: 2950-2956.
64. Brooijmans, R. J. W., De Vos, W. M., Hugenholtz, J., (2009). "Lactobacillus plantarum WCFS1 Electron Transport Chains", *Applied and Environmental Microbiology*, 75: 3580-3585